

# Environmental Research Letters



## LETTER

# Extreme multi-basin flooding linked with extra-tropical cyclones

### OPEN ACCESS

#### RECEIVED

29 March 2017

#### REVISED

20 July 2017

#### ACCEPTED FOR PUBLICATION

16 August 2017

#### PUBLISHED

1 November 2017

Original content from this work may be used under the terms of the [Creative Commons Attribution 3.0 licence](#).

Any further distribution of this work must maintain attribution to the author(s) and the title of the work, journal citation and DOI.



Paolo De Luca<sup>1,4</sup> , John K Hillier<sup>1</sup>, Robert L Wilby<sup>1</sup>, Nevil W Quinn<sup>2</sup> and Shaun Harrigan<sup>3</sup>

<sup>1</sup> Department of Geography - Loughborough University, Loughborough, United Kingdom

<sup>2</sup> Department of Geography and Environmental Management - University of the West of England, Bristol, United Kingdom

<sup>3</sup> Centre for Ecology & Hydrology (CEH), Wallingford, United Kingdom

<sup>4</sup> Author to whom any correspondence should be addressed.

E-mail: [p.deluca@lboro.ac.uk](mailto:p.deluca@lboro.ac.uk)

**Keywords:** multi-basin, flooding, extra-tropical cyclones, Great Britain, emergency management, interactions, natural hazards

Supplementary material for this article is available [online](#)

## Abstract

Fluvial floods are typically investigated as ‘events’ at the single basin-scale, hence flood management authorities may underestimate the threat of flooding across multiple basins driven by large-scale and nearly concurrent atmospheric event(s). We pilot a national-scale statistical analysis of the spatio-temporal characteristics of extreme multi-basin flooding (MBF) episodes, using peak river flow data for 260 basins in Great Britain (1975–2014), a sentinel region for storms impacting northwest and central Europe. During the most widespread MBF episode, 108 basins (~46% of the study area) recorded annual maximum (AMAX) discharge within a 16 day window. Such episodes are associated with persistent cyclonic and westerly atmospheric circulations, atmospheric rivers, and precipitation falling onto previously saturated ground, leading to hydrological response times <40 h and documented flood impacts. Furthermore, peak flows tend to occur after 0–13 days of very severe gales causing combined and spatially-distributed, yet differentially time-lagged, wind and flood damages. These findings have implications for emergency responders, insurers and contingency planners worldwide.

## 1. Introduction

Floods endanger lives, damage the built environment, cause disruption and accrue significant economic losses. The Sendai Framework for Disaster Risk Reduction [1] recommends better mapping and management in areas prone to flooding to increase resilience through public and private investment in disaster risk prevention and reduction measures. The UK Climate Change Risk Assessment [2] highlighted that flood risks are already significant in the UK and are expected to rise as a consequence of climate change. Pragmatic and well-targeted actions were called for with respect to high magnitude flood risks for communities, businesses and infrastructures [2]. Anecdotally, high-magnitude flood episodes also tend to impact large areas covering multiple river basins [3–6].

To date, fluvial flooding has tended to be studied on a basin-by-basin basis with respect to physical processes and impacts [7–15]. Some statistical methods for

creating design floods rely on pooled data from multiple basins [16, 17], but these approaches are indifferent to any spatial and temporal relationships in the data, whereas multivariate extreme value statistics are useful for estimating return periods for major events [18–20] and for characterizing spatially varying and time-lagged extreme flows [21–23]. Within the reinsurance sector, weather-driven multi-basin ‘catastrophe models’ are widely used to estimate economic losses due to flooding [24, 25]. Statistical approaches to joint probabilities [21, 22, 26–29] have been extended to multi-basin flooding (MBF), as well as simulation of extreme flow events for northeast England using conditional probability models [30]. Historical MBF episodes have also been investigated in Germany [31, 32], and across Europe climate models have been used to project economic losses [e.g. 33]. However, so far in Great Britain (GB) and elsewhere, there have been no national-scale analyses using simple and pragmatic statistics that specifically focus on the spatio-temporal

characteristics of extreme MBF and their links with extra-tropical cyclones (ETCs), that are known to affect the most extreme single-basin floods [34].

The MBF approach here proposed overcomes the limitations of single-basin return period estimation, with the possibility of developing a national-scale return period for improved risk communication. A MBF episode can simultaneously impact very large regions, with the chance to overwhelm emergency responses, e.g. coordinated by the UK Environment Agency. In addition, MBF may coincide with ETCs, which together create a multi-peril scenario of flood-wind impacts. Such episodes may be more severe than what planned for; illustratively, combined flood-wind impacts at the 16 year return period are increased by the link between perils, costing an additional £0.3 billion for domestic UK properties [35].

We present a pragmatic approach for detecting and quantifying the characteristics of extreme MBF episodes and their links with ETCs. We use GB as pilot area, but deploy techniques that are applicable wherever there are gauged river flow data. We searched a window of 1 to 19 days for coincident peak flow annual maxima (AMAX) in 260 non-nested river basins during the 1975–2014 period. Following sections describe the data, methodological approach and metrics, then the six most extensive and temporally distinct MBF episodes identified. We confirm that these most extensive MBF had widespread impacts [36–42] and mostly occurred during winter. A particularly powerful aspect of our approach is that it is compatible with the synoptic-scale (i.e.  $\sim 1000$  km horizontal length scale) of atmospheric conditions and land-surface properties. This allows severe MBF episodes to be evaluated alongside categories of atmospheric circulation (Lamb weather types, LWTs), antecedent rainfall as a proxy for soil moisture (Standardized Precipitation Index, SPI), atmospheric rivers (ARs), and storminess (very severe gale, VSG, frequency). Moreover, the hydrological response (joining time,  $Jt$ ) for large and small basins is examined to determine lagged responses in the system. Finally, the causes and implications of extreme MBF and their relationship with ETCs are discussed.

## 2. Peak flow data

Highest instantaneous (15 min) peak flows ( $\text{m}^3\text{s}^{-1}$ ) in each water year (1st October–30th September) were extracted from the 1975–2014 record. These annual maxima (AMAX) series were drawn from 260 gauged basins widely distributed across Great Britain (GB), within a 40 year block that provides the best compromise between spatial and temporal coverage. Our network of stations is non-nested (i.e. one gauge per basin) and covers 60.1% of GB land area (figure 1). This is equivalent to Network A used in a previous related study [43] but with more representative coverage across GB. The mean

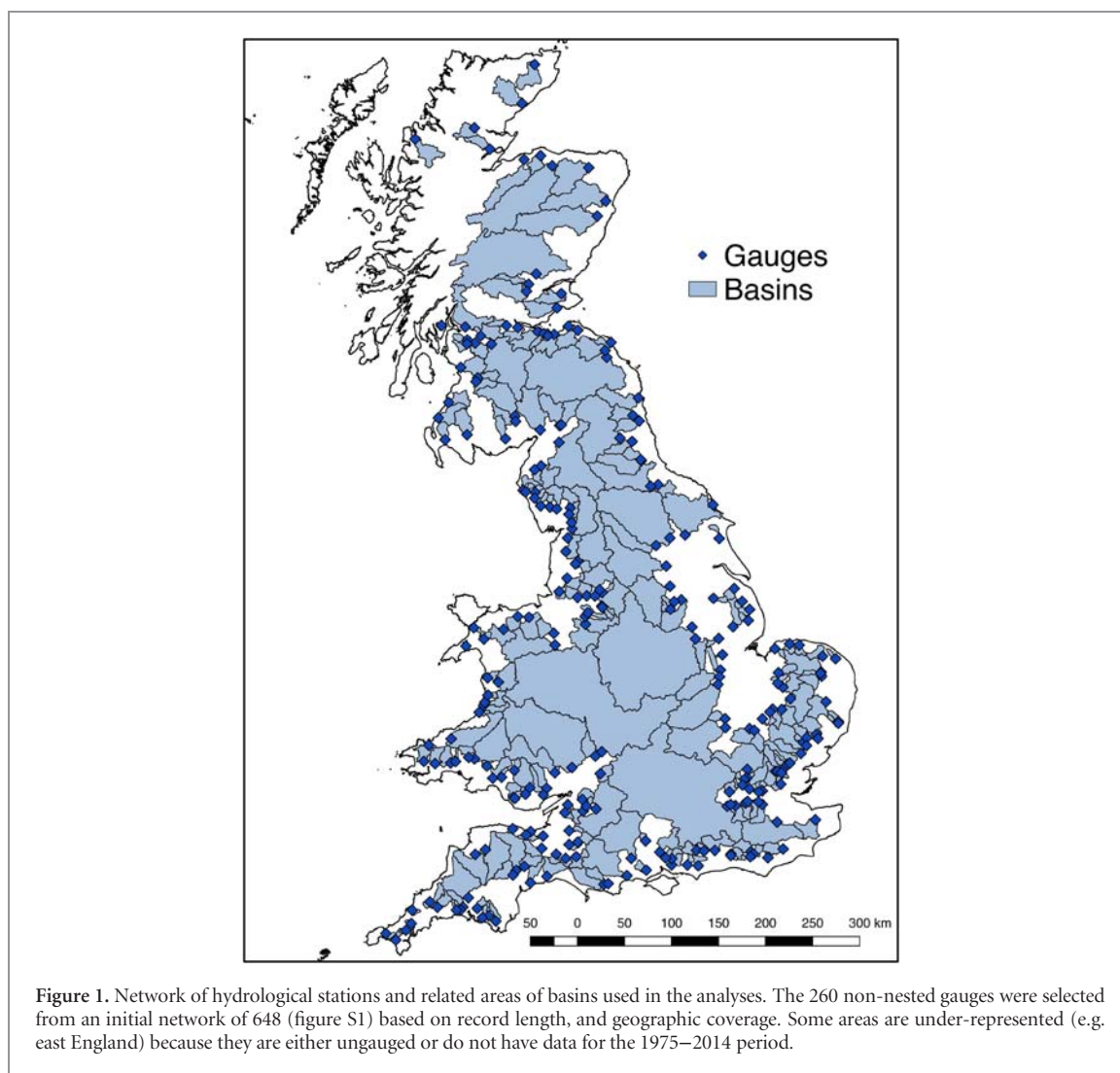
basin area ( $A$ ) is  $484 \text{ km}^2$ , ranging from  $12 \text{ km}^2$  (Pointon Lode) to  $9948 \text{ km}^2$  (Thames), and average basin elevation is 149 m a.s.l. Data were obtained from the National River Flow Archive using WINFAP-FEH v4.1: <http://nrfa.ceh.ac.uk/content/winfap-feh-files-version-history> and, for Scotland, from the Scottish Environment Protection Agency.

## 3. Methods

A pragmatic metric that defines the hydrological severity of a multi-basin flooding (MBF) episode, particularly one that highlights the spatial distribution of basins involved, is not yet available. So far, the severity of a single-basin fluvial flow is readily defined by the peak discharge, and it is also possible to rank MBF severity using the most extreme peak flow of the basins under study [23, 29]. Alternatively, severity may be defined in terms of economic impact [33, 35], but complete and comparable residential and commercial loss estimates are extremely difficult to obtain for all but the most severe historical events. Recent studies have begun to assess the severity of flooding episodes by considering the whole UK, effectively extending the paradigm applied to single-basin floods by looking at monthly mean river flows [3, 12] and seasonal river flow accumulations [4].

The MBF metrics proposed here are based on a deliberately straightforward procedure that counts the total number of basins involved in each episode. Our principal metric, denoted  $n_g$ , uses the summed number of independent gauges that report a peak flow annual maximum (AMAX) within a given multi-day time window ( $L$ ). This extends a previous single-day approach [43] to include MBF episodes where AMAX fall within a window of length of  $L$  days from 1 up to 19, ending on the day where most gauges report their AMAX, denoted  $d_{\text{max}}$ .

The following procedure was implemented (R code in supplementary data available at [stacks.iop.org/ERL/12/114009/mmedia](https://stacks.iop.org/ERL/12/114009/mmedia)) to identify MBF and determine their  $n_g$ . Firstly, for each day  $j$  determine  $n_{g,j}$  and list these in descending order, creating the list of MBF episodes for  $L = 1$  day. Then for each  $L > 1$ , using episodes of the  $L = 1$  day list anew for each  $L$ , follow these 4 steps: (1) ascertain that the current episode ( $C$ ) is the largest (i.e. greatest 1 day  $n_g$ ) as yet un-amalgamated remaining on the list; (2) identify any other basins reaching their AMAX within the specified time window before  $C$ ; (3) add all their  $n_{g,j}$  to  $C$ 's count and flag the smaller episodes as being amalgamated with  $C$ , which prevents any day contributing to more than 1 episode for a given  $L$ ; (4) repeat (1)–(3) until no more amalgamation is possible. Hence, when considering the  $n_g$  metric, the most extreme MBF episode is defined as that with the greatest number of basins exhibiting near concurrent AMAX within the specified time window ( $L$ ). However, two other characteristics



were derived for each episode. These are: (i) the multi-basin Flood Yield ( $mFY$ , supplementary data A); and (ii) the total drained area ( $TDA$ ) of the basins reaching their AMAX within an episode. These use the same list of episodes, and basins, defined by the  $n_g$  metric, but an alternative quantity to rank severity. The  $mFY$  index is potentially biased towards small basins, whereas  $TDA$  intrinsically assigns greater weight to larger basins.

The AMAX dates for individual river basins are denoted event set A. Event set B comprises extreme MBF episodes with severity defined in terms of  $n_g$ , taking the largest temporally distinct episodes defined by six key time windows with different lengths, varying from 1 to 16 days (figure 2, table 1), and the 10 next largest episodes in each key time window. Event set C contains the most extreme  $L = 13$  days MBF episode for each water year defined using  $mFY$ , and set D is similar except defined by  $TDA$ . Event set E consists of the six most extreme episodes defined by  $n_g$  (figures 2, 3(a) and (b), table 1). Replicated days are removed such that days occurring in two or more window lengths' episodes, necessary only in B and

E, are never counted twice. Similarly, days with  $>1$  single-basin AMAX are not counted repeatedly for national-scale analyses (figures 3(c) and (d)). Where different observations need to be shown basin-by-basin, multiple basins recording their AMAX are permitted to contribute on the same day (figure 4).

## 4. Results

### 4.1. Characterizing severe multi-basin flooding (MBF) episodes

The most extreme multi-basin flooding (MBF) episodes defined by  $n_g$ , i.e. by the concurrent number of basins reaching their peak flow annual maxima (AMAX), obtained from 19 time window lengths ( $L$ ), comprise five temporally distinct episodes (event set E, figure 2 and table 1). These are:  $d_{\max} = 27/12/1979$  (66 basins involved, 18.6% of study area, window length  $L = 1$  day);  $30/10/2000$  (68, 14.1%,  $L = 2$  days);  $01/01/2003$  (75, 24.9%,  $L = 4$  days);  $02/12/1992$  (96, 22%,  $L = 8$  days); and  $01/02/1995$  (108, 46.5%,  $L = 16$  days), with  $d_{\max}$  representing the day, in each episode, where

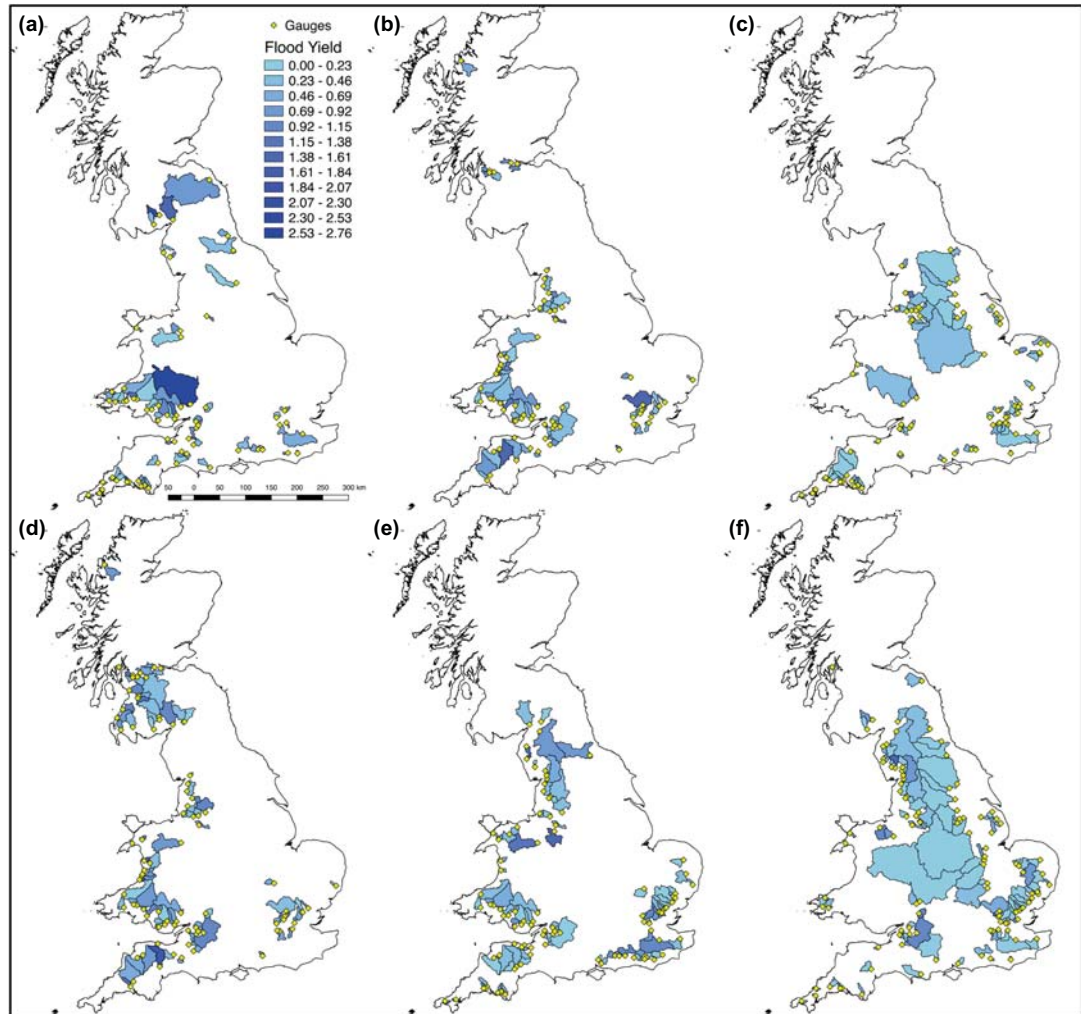


**Figure 2.** Distribution of basins contributing to the extreme multi-basin flooding (MBF) episodes in Great Britain (GB) during 1975–2014 for six time window lengths ( $L$ , event set E). The maps show respectively: (a)  $L = 1$  day ( $d_{\max} = 27/12/1979$ ); (b)  $L = 2$  days ( $d_{\max} = 30/10/2000$ ); (c)  $L = 4$  days ( $d_{\max} = 01/01/2003$ ); (d)  $L = 6$  days ( $d_{\max} = 30/10/2000$ ); (e)  $L = 8$  days ( $d_{\max} = 02/12/1992$ ); and (f)  $L = 16$  days ( $d_{\max} = 01/02/1995$ ). Flood Yield (FY) is a severity metric that represents each basin's peak flow annual maximum (AMAX) normalized by the relative basin area ( $A$ ) and  $d_{\max}$  is defined as the day where the largest number of AMAX have been registered within each episode.

the largest number of AMAX have been recorded. If different time windows return the same date, the window with the largest number of concurrent AMAX is given. However, the  $L = 6$  days episode (30/10/2000, figure 2(d), table 1) is included because the number of basins involved (86) and total drained area (TDA, 24 971 km<sup>2</sup>) are both much larger than the  $L = 2$  days episode. Figure 2 shows the regional distribution and basin-by-basin Flood Yield (FY, supplementary data A) severity of these six episodes.

The  $n_g$  metric ranges from 66 ( $L = 1$  day) to 108 ( $L = 16$  days), plateauing at  $L \cong 13$  days (figure 3(a)). For all time windows, the number of co-occurrences is notably larger than expected by chance ( $p < 0.01$ , binomial test, supplementary data F.1). The TDA ranges from 17 787 km<sup>2</sup> ( $L = 2$  days) to 58 491 km<sup>2</sup> ( $L = 16$  days), again plateauing at  $L \cong 13$  days (figure 3(b)). These areas correspond to a TDA percentage of 14.1% and 46.5% of the area of the 260 gauged basins

respectively, or 8.5% and 27.9% of the total land area of Great Britain (GB, figure 3(b), table 1). Window length  $L = 13$  days is used to define event sets C and D as it captures the largest episodes whilst retaining the maximum temporal resolution.

Figure 3(c) shows that the six most extensive MBF episodes (event set E) tended to occur during the winter (December–February), closely matching the pattern of event sets A–D. However, AMAX occurrences in January are more common for MBF episodes (event sets B–E) than for single-basin events (event set A). Spatially, event set E episodes impacted a substantial proportion of our study basins (figures 2 and 4(d)). However, when considering more episodes (event sets B–D) the spatial distribution of basins impacted is even larger, with all the study area affected (figures 4(a), (b) and (c)). Figure 4 shows also that the relative frequency of AMAX occurrences is homogeneously distributed across all the basins for

**Table 1.** Extreme multi-basin flooding (MBF) episodes in Great Britain (GB) during 1975–2014 (event set E). Observations are derived from 19 time windows up to 18 days prior to  $d_{\max}$  (i.e. the day where the largest number of peak flow AMAX have been registered). See main text for details. (a) Window length ( $L$ ) in days; (b) Total drained area ( $TDA$ , km<sup>2</sup>) involved in each episode (i.e. sum of the areas of all involved basins); (c)  $TDA$  percentage (%) of the 260 basins affected within each episode; (d) Percentage (%) of GB land area affected within each episode; (e) Dates of episodes, where the top row is  $d_{\max}$ ; (f) Number of basins with AMAX registered within each distinct day; (g) Total number of basins with AMAX registered within each distinct episode; (h) Percentage (%) of total number of basins (out of 260) with concurrent AMAX per episode; (i) Daily Lamb weather type (LWT); (j) Average joining time ( $Jt$ , in days), within an episode, for larger basins ( $A \geq 1000$  km<sup>2</sup>); (k) Average  $Jt$  for small basins ( $A < 1000$  km<sup>2</sup>). In (j) and (k) uncertainties are 1 standard error.

(a) Time window length ( $L$ , days)	(b) Total drained area ( $TDA$ , km <sup>2</sup> )	(c) Total drained area ( $TDA$ , %)	(d) GB area %	(e) Date	(f) No. basins per day	(g) No. basins per episode	(h) No. basins %	(i) LWT	(j) Average joining time ( $A \geq$ 1000 km <sup>2</sup> )	(k) Average joining time ( $A <$ 1000 km <sup>2</sup> )
1	23 399	18.6	11.18	27/12/1979	66	66	25.3	C	–	–
2	17 787	14.1	8.50	30/10/2000 29/10/2000	62 6	68	26	C CSW	2	1.91 ± 0.0
4 (3 & 5 same $d_{\max}$ as 4)	31 370	24.9	14.99	01/01/2003 31/12/2002 30/12/2002 29/12/2002	34 7 29 5	75	28.7	C S C C	2.83 ± 0.3	2.94 ± 0.1
6	24 971	19.8	11.93	30/10/2000 29/10/2000 28/10/2000 27/10/2000 26/10/2000 25/10/2000	62 6 0 2 0 16	86	33	C CSW C W W NW	5 ± 1	4.93 ± 0.2
8 (7 same $d_{\max}$ as 8)	27 674	22.0	13.22	02/12/1992 01/12/1992 30/11/1992 29/11/1992 28/11/1992 27/11/1992 26/11/1992 25/11/1992	49 1 19 2 0 5 17 3	96	36.8	C SW SW S ANE SW W SW	7 ± 0.8	5.91 ± 0.3
16 (9 to 15 & 17 to 19 same $d_{\max}$ as 16)	58 491	46.9	27.94	01/02/1995 31/01/1995 30/01/1995 29/01/1995 28/01/1995 27/01/1995 26/01/1995 25/01/1995 24/01/1995 23/01/1995 22/01/1995 21/01/1995 20/01/1995 19/01/1995 18/01/1995 17/01/1995	19 16 9 9 10 16 14 3 2 3 3 1 2 0 0 1	108	41.4	W SW ANE C C S N C W CNW C C CS SW CS	13.73 ± 0.9	11.97 ± 0.3

all event sets considered, possibly excluding Scotland for set E. This contrasts with precipitation distributions during winters dominated by westerly or cyclonic patterns [44], when rainfall tends to respectively decrease from west-to-east or is heavier in the east.

The average joining time ( $Jt$ , supplementary data B) for larger ( $A \geq 1000$  km<sup>2</sup>) and smaller ( $A < 1000$  km<sup>2</sup>) basins within MBF episodes was compared. Considering time windows ( $L$ ) separately for event set E (figure S3), only when  $L = 2$  or 16 days do larger basins join significantly later than small ones ( $t$ -test non-paired, supplementary data F.2), and the delays were modest, just 0.1 and 1.8 days respectively

(table 1). Event sets B-D replicate this, showing occasional significance but a difference in  $Jt < 48$  h. A time to peak ( $T_p$ ) response analysis (supplementary data C) [45, 46] for larger basins further indicates  $T_p < 40$  h, again less than the ~13 day time-span that appears to define extreme MBF episodes.

#### 4.2. Relationship to inundation episodes

Severity measured by  $n_g$  is a proxy for overbank flow and fluvial flood extent. Only a fraction of the basins' areas will actually be inundated. However, the six extreme MBF episodes (event set E, figure 2) all resulted in widespread flooding demonstrating the relevance of the  $n_g$  metric as a diagnostic:

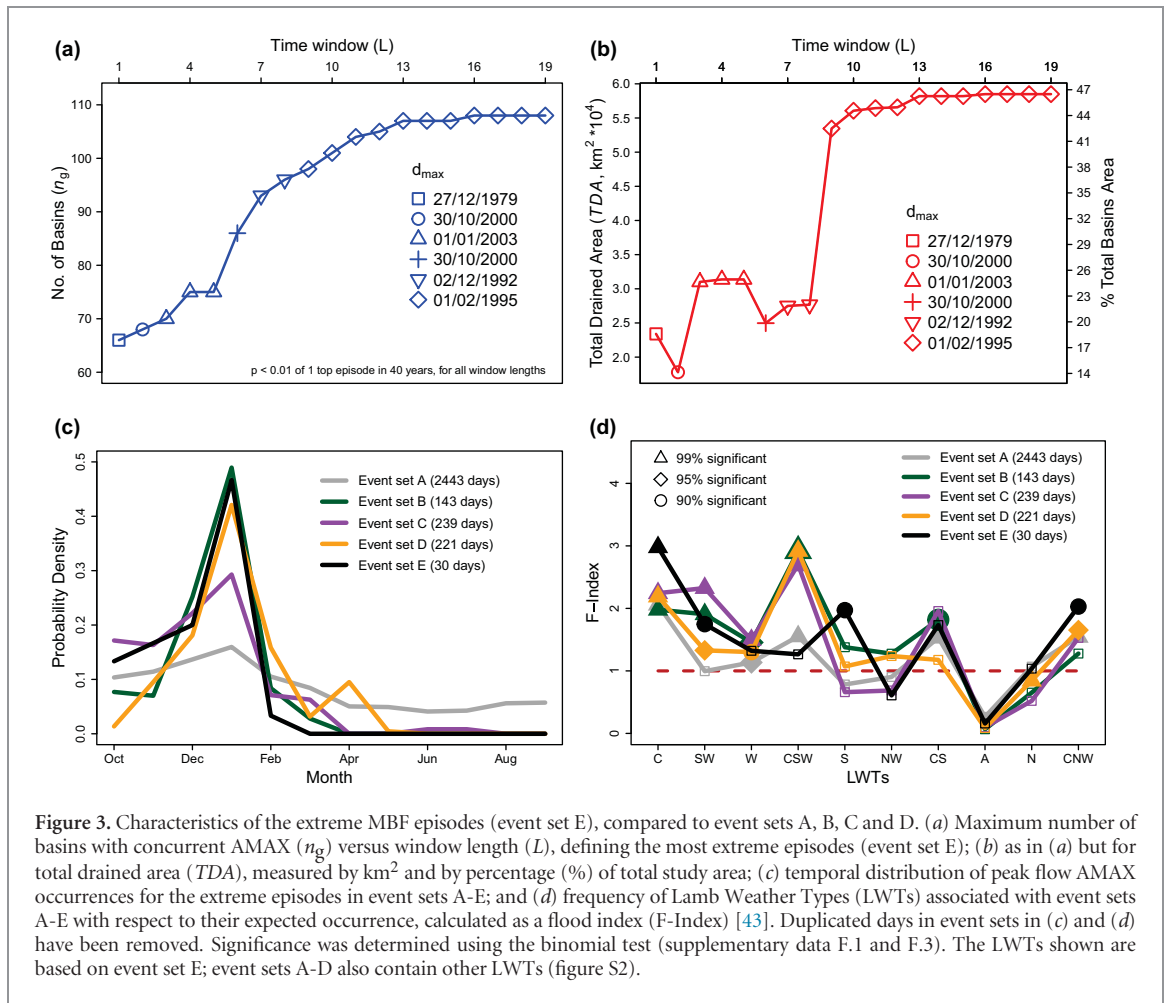


**Figure 3.** Characteristics of the extreme MBF episodes (event set E), compared to event sets A, B, C and D. (a) Maximum number of basins with concurrent AMAX ( $n_g$ ) versus window length ( $L$ ), defining the most extreme episodes (event set E); (b) as in (a) but for total drained area (TDA), measured by  $\text{km}^2$  and by percentage (%) of total study area; (c) temporal distribution of peak flow AMAX occurrences for the extreme episodes in event sets A-E; and (d) frequency of Lamb Weather Types (LWTs) associated with event sets A-E with respect to their expected occurrence, calculated as a flood index (F-Index) [43]. Duplicated days in event sets in (c) and (d) have been removed. Significance was determined using the binomial test (supplementary data F.1 and F.3). The LWTs shown are based on event set E; event sets A-D also contain other LWTs (figure S2).

- The December 1979 episode (figure 2(a)) was the most severe in South Wales since 1960 and in some areas the worst in a century, causing extensive floods that killed four people, necessitated the evacuation of hundreds and caused millions of pounds of damage [36].
- The Autumn 2000 episodes (figures 2(b) and (d)) were described as the most devastating in England since 1947, and associated with the wettest 12 month period since 1776 [37, 38].
- The January 2003 episode (figure 2(c)) was reported by the Environment Agency in *FloodLink* [39] with most severe floods in the East Midlands, where the Trent basin had 118 flood warnings and 14 flood watches issued between 29/12/2002 and 03/01/2003.
- The November/December 1992 episode (figure 2(e)) was reported by the UK Met Office [40] after floods impacted southern England during the night of 25th/26th November. However, the worst phase occurred on the 29th, when flooding in Wales devastated homes and caused widespread road and railway disruptions.
- The February 1995 episode (figure 2(f)) caused severe floods on at least 7 rivers, following heavy frontal precipitation in January 1995 which was 79% above the 1961–1990 average [41, 42].

#### 4.3. Relationship to atmospheric patterns

Daily UK synoptic-scale atmospheric patterns are characterized by Lamb weather types (LWTs) [47, 48]. The frequency of LWTs for days during extreme single- and multi-basin peak flow episodes was compared with the entire 40 year catalogue of LWTs (figure 3(d)). In this comparison, a flood index (F-Index, supplementary data D) [43] is defined as the ratio of observed to expected frequency of LWTs. This was undertaken for event sets: A (2443 days), B (143 days), C (239 days), D (221 days) and E (30 days), excluding replicate dates. Statistical significance of the F-Index was calculated using a binomial test (supplementary data F.3).

Overall, the cyclonic (C-type) LWT is strongly associated with the peak flows with a 99% statistically significant F-Index  $\geq 1.98$  for all event sets considered, in particular flooding was  $\sim 3$  times more likely than expected during C-type occurrences for event set E. The south-westerly (SW), westerly (W), and cyclonic SW (CSW) types are also associated with AMAX events ( $p < 0.01, 0.05$  and  $0.1$ ), and therefore more likely linked with widespread flooding. Southerly (S) types are significantly represented in event sets E, but not in event sets A-D (figure 3(d)). Therefore, a pattern of C- and W-types contributing to widespread peak flows is depicted and the multi-basin event sets B-E show very

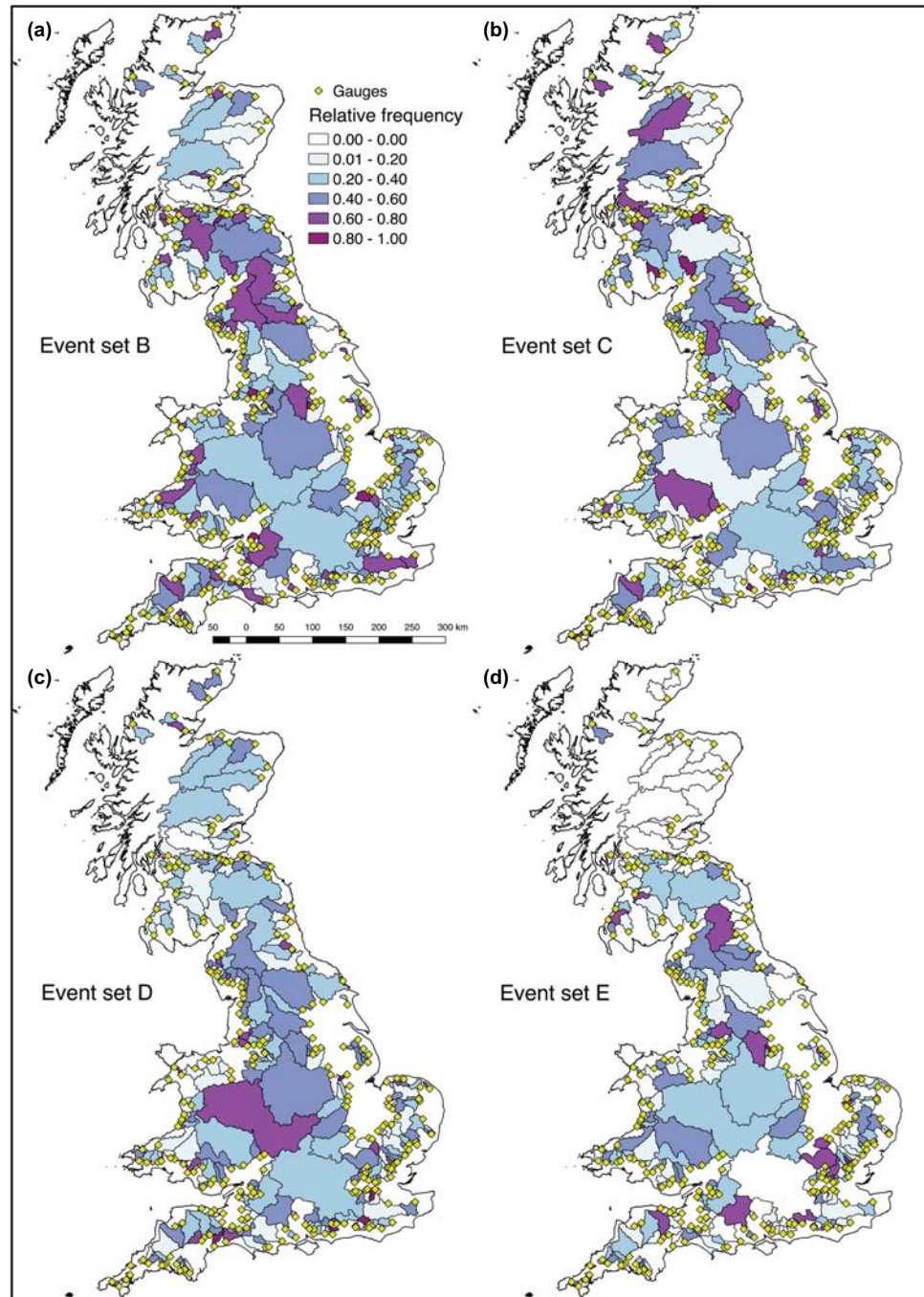


**Figure 4.** Distribution and relative frequency of occurrence of peak flow annual maxima (AMAX) within event sets B, C, D and E. (a) Event set B; (b) event set C; (c) event set D; and (d) event set E. The colour scale is a ratio (i.e. from 0 to 1) of AMAX occurrences in a given basin relative to the basin with the largest number in that panel, with dark colours indicating most occurrences.

similar F-Index results when compared to single-basin AMAX (event set A, figure S4).

It is also of interest if these circulation systems are particularly ‘wet’. Atmospheric rivers (ARs) are corridors of intense horizontal water vapour transport within the warm conveyor belt of extra-tropical cyclones (ETCs) [34, 49]. The dates of event set E episodes are compared with the Brands *et al* AR archive [50] derived from ERA-Interim reanalysis [51]. Four out of the five temporally distinct MBF episodes’ most extreme flows (i.e.  $d_{\max}$  dates) occurred on the same day as an AR, which on average happen on only 30%

of extended (October–March) winter days ( $p < 0.01$ , binomial test, supplementary data F.4).

#### 4.4. Relationship with antecedent soil moisture conditions

Wet soil moisture antecedent conditions increases the likelihood of flooding [52]. The standardized precipitation index (SPI, supplementary data E) [53, 54] is widely used as a proxy for this physical property and 3–24 month SPI values are distinctively high for historical flooding episodes [55–57]. Whilst the sample of

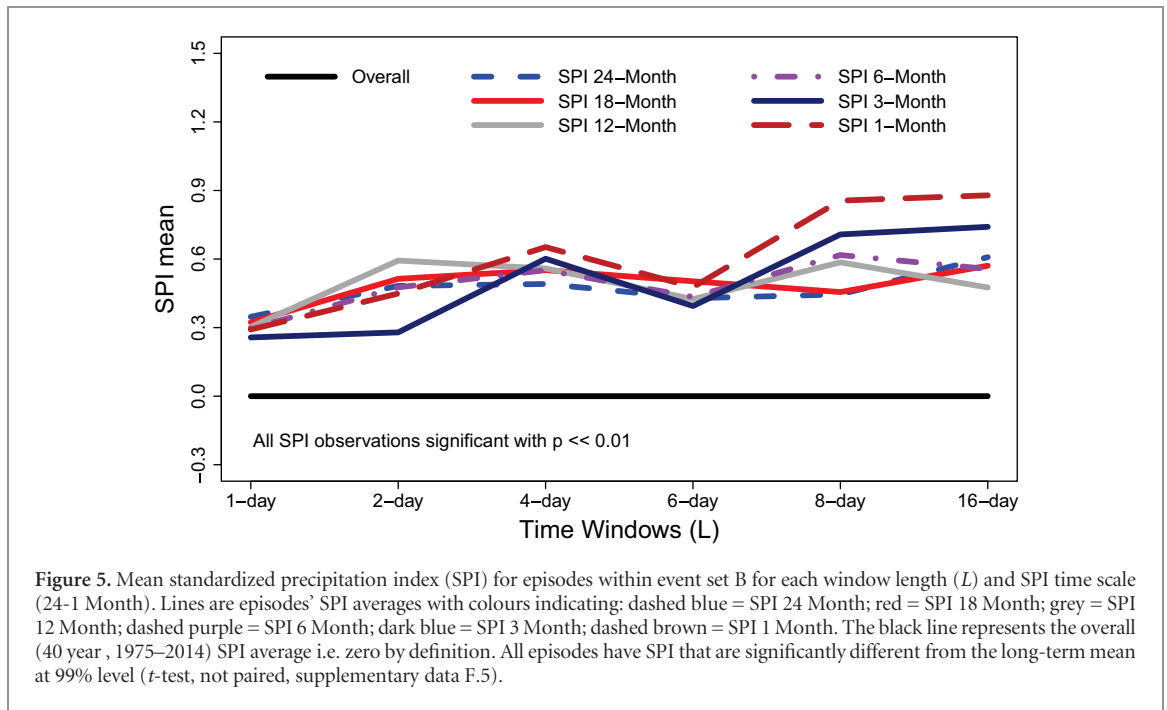


**Figure 5.** Mean standardized precipitation index (SPI) for episodes within event set B for each window length ( $L$ ) and SPI time scale (24-1 Month). Lines are episodes' SPI averages with colours indicating: dashed blue = SPI 24 Month; red = SPI 18 Month; grey = SPI 12 Month; dashed purple = SPI 6 Month; dark blue = SPI 3 Month; dashed brown = SPI 1 Month. The black line represents the overall (40 year, 1975–2014) SPI average i.e. zero by definition. All episodes have SPI that are significantly different from the long-term mean at 99% level ( $t$ -test, not paired, supplementary data F.5).

episodes in event set E is too small to show a pattern, SPI aggregated across impacted basins [58] is higher than average across all window lengths ( $L$ ) for event set B ( $p \ll 0.01$ ,  $t$ -test non-paired, supplementary data F.5), increasing with  $L$  (figure 5). Event set C, based on the multi-basin flood yield ( $mFY$ ) metric, by incorporating a forced regularized annual sampling, demonstrates that flood magnitude is greater in 'wet' spells ( $SPI > 0.5$ ) than 'dry' periods ( $SPI < -0.5$ ) with mean  $mFY = 26.9 \pm 3.4$  ( $1\sigma$ ) and  $17.1 \pm 1.3$  ( $1\sigma$ ) as calculated from SPI 12 Month. Indeed, for this comparison, all except SPI 1 Month are significant ( $p < 0.05$ ,  $t$ -test, 2-tailed). Event set D (based on  $TDA$ ) shows no signal for this well-established flood-SPI connection, suggesting that the metric based on  $mFY$  might better reflect physical processes.

#### 4.5. Relationship to very severe gales

Flooding and severe wind have been reported for some ETCs impacting western Europe [3, 59]. A potential association between extreme MBF and severe storms was, therefore, investigated. In a year-by-year analysis the most extreme  $L = 13$  days  $mFY$  episodes (event set C) correlates positively with the number of days with very severe gales (VSG) as defined by the Jenkinson Gale Index [48] in that year ( $r = 0.41$ ,  $p = 0.0088$ , 2-tailed  $t$ -test, supplementary data F.6) (figure 6). Taking the most severe 50% and 30% of years for wind and flow respectively, co-occurrence is expected 6.0 times in 40 years, but 10 are observed ( $p = 0.021$ ; Monte Carlo simulation with  $n = 10000$ ), making coincidence of extremes 67% more likely than what would be expected by chance.

Furthermore, the timing of these episodes is the basis for insights into the physical processes at work. For 5 out of 10 observed co-occurrences, the most extreme

peak flows recorded on  $d_{\max}$  are on a day with VSG, and 9 of 10 peak flows are within 0–13 days after a VSG day ( $p \ll 0.001$ , binomial test). This contrasts with 0 out of 10 peak flow episodes found in the preceding 0–13 days of a VSG day. In agreement with the flood-SPI analysis, the relationship is notably less strong for event set D (based on  $TDA$ ), indicating that  $mFY$  may better reflect physical processes in storm systems.

Wet ground is a pre-requisite to the most severe peak flow episodes, but there is also a link with gales. Six out of the 10 most severe episodes have a SPI 12 month between +0.4 and +1.1 (figure 6, white circles), whereas less severe episodes tend to show a negative SPI (figure 6, black circles). The two outliers in figure 6 (1983 and 2014) reflect previous studies [4, 44, 60–63] that showed that the number of cyclones were particularly high over the GB during these years. However, the largest  $mFY$  for these two episodes may be depressed by the AMAX measure of extremeness which, by definition, limits the number of occurrences per year. Therefore, these observations are likely valid given, if influenced by the analytical method used.

## 5. Discussion

### 5.1. A new multi-basin approach

We have presented various diagnostics for the evaluation of multi-basin flooding (MBF) episodes. The first metric ( $n_g$ ) detects key 'episodes' by summing the concurrent number of basins attaining their peak flow annual maximum (AMAX) within a given time window ( $L$ ), then ranking the episodes based on  $n_g$ . We also considered episodes ranked by total drained area ( $TDA$ ) and multi-basin flood yield ( $mFY$ ). When episodes are identified in terms of  $n_g$ , this gives perhaps

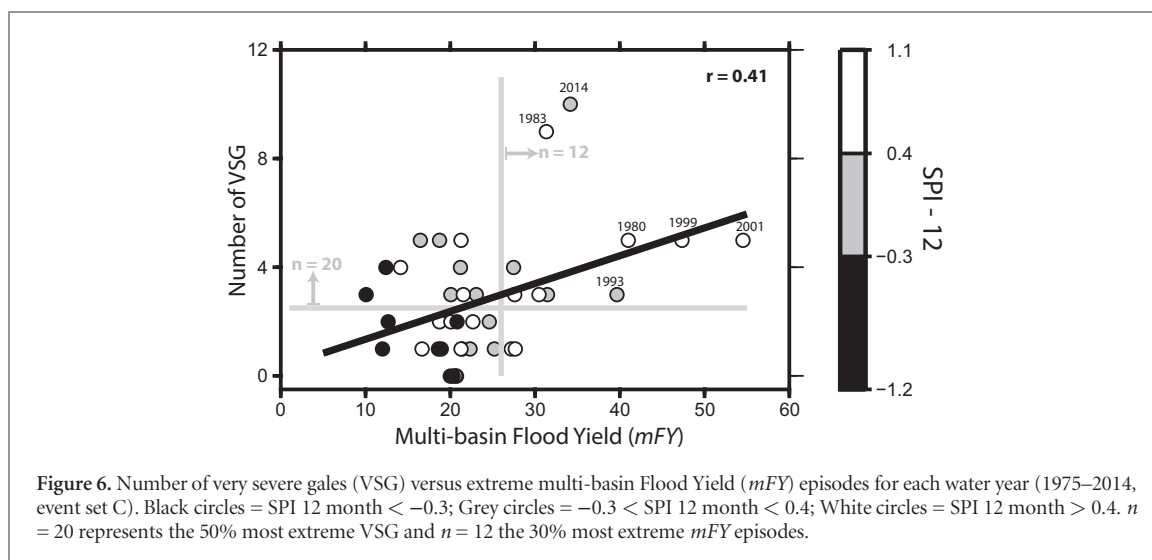


**Figure 6.** Number of very severe gales (VSG) versus extreme multi-basin Flood Yield (*mFY*) episodes for each water year (1975–2014, event set C). Black circles = SPI 12 month < -0.3; Grey circles = -0.3 < SPI 12 month < 0.4; White circles = SPI 12 month > 0.4.  $n = 20$  represents the 50% most extreme VSG and  $n = 12$  the 30% most extreme *mFY* episodes.

undue weight to small basins, but *TDA* emphasizes larger rivers. The *mFY* can either weight small basins, when calculated as here or large ones if area and flow were each summed before dividing them. All are practical options, but awareness of any biases and use of multiple metrics is recommended to ensure robust insights.

There are various advantages with this approach to MBF analysis. First, because of the different time windows ( $L$ ) used within each metric, it enables the identification of extreme peak flow episodes that are driven by persistent rain-bearing weather systems by accounting for variations in time-lags between precipitation and peak flows, that depend on rainfall properties, basin area and geology. Second, it provides a national-scale flood measure allowing more meaningful comparison with synoptic-scale weather patterns than at the scale of individual basins, regardless of the catchment area [35]. Third, whichever metric is selected a return period that is applicable across a whole country can be estimated.

A single, national rather than basin-scale, return period has a potentially important role in risk communication. Such metrics could address the question often posed by flood managers: ‘Why is there a 1 in 100 year flood event every year?’ This impression arises because return period estimates are traditionally based on flows at a single gauge. The MBF metrics proposed here would yield the 1-in-100 year episode based on a return period estimate that integrates information across all basins in a network.

## 5.2. Widespread concurrent impacts

Our results show that extreme MBF episodes affect large areas (figure 2), with likely commensurate damages [36–42]. For instance, the  $L = 16$  days episode captures ~46% of the study area, or ~27% of Great Britain (GB), with 108 basins concurrently reaching their AMAX (figures 2(f), 3(a) and (b), table 1). Aspects of the physical processes driving these widespread episodes appear

similar to those deduced from single-basin studies [3, 4, 7, 8, 11–13, 15, 44]. First, W- and C- Lamb weather types (LWTs) associated with MBF (figure 3(d), table 1) have been linked to frequent floods [43, 64], the wettest winters in England and Wales [44], and >80% of extreme flows on the River Eden (UK) [64]. The W-type, in particular, represents one of the main drivers of high rainfall and flows in the UK [64, 65] as well as flooding throughout central Europe [e.g. 64]. Second, MBF is larger (by *mFY*) in wet years, i.e. when the SPI > 0.5, and in longer time windows when the SPI is higher, suggesting antecedent soil moisture conditions may play a role. Third, as for single-basin floods [34], the most extreme MBF episodes coincide with atmospheric rivers (ARs).

The observation that single-basin flooding in GB occurs mostly during winter also applies to MBF (figure 3(c)). This is due to frequent storms and their associated precipitation [66], combined with lower evapotranspiration, and wetter antecedent soil conditions (figure 5) that ultimately combine to generate higher flows [11, 12]. However, compared to single-basin flooding, the largest MBF are even more strongly typified by occurrence in January (figure 3(c)), when the most favourable atmospheric flood-generating conditions (C, SW, W and CSW circulation types) are more likely. This close association with synoptic weather is not surprising, but neither it is required by or self-evident *a priori* from single-basin analyses.

A key feature that distinguishes large MBF from their single-basin counterparts is their duration (i.e.  $\cong 13$  days, figures 3(a) and (b)). This is greater than currently accounted for in other studies [28], and indicates that at least one notable source of persistence or ‘memory’ in the physical system is required. With a time to peak ( $T_p$ ) < 40 h [45, 46], these sources cannot be within the channelized flow paths, a view supported empirically by larger basins joining episodes at essentially the same time as smaller ones (table 1, figure S3). This observation also rules out, from the possible sources of ‘memory’, reservoirs delaying flow outside

of the channels, and is reconciled by the fact that concentration time increases with basin area [67]. Thus, we postulate that a ‘memory’ exists in either antecedent soil or groundwater levels [55–57] (figure 5) and/or in persistent atmospheric patterns during notably wet years [3, 4, 12, 44, 59, 61], such as known ETCs clustering in extreme winters [63]. These elements of ‘memory’ likely exist for larger European rivers (e.g. Rhine), although they are less easily decoupled because time-scales attributable to the processes overlap more.

### 5.3. Compounding flood and wind impacts

Extra-tropical cyclones (ETCs) were identified as a driver of MBF, firstly via an association with cyclonic LWTs and ARs. Also, when considering these high flows in terms of extreme *mFY* for each water year within  $L = 13$  days (event set C), a relationship with damaging winds predominantly caused by ETCs is also demonstrated. A significantly positive correlation exists between VSG and MBF, with co-occurrence of extremes 67% more likely than by chance and high flows occurring within 0–13 days after a VSG day. Hence, building on case studies of notable years [4, 12, 13, 44, 61, 62] and the Trent basin in central England [35], this is the first systematic, national-scale evidence that the severest aspects of wet and windy winters tend to co-occur and are linked by the physical processes associated with ETCs. Often these phenomena are viewed separately: severe ETCs bring extreme winds [68] whilst slower moving, less windy ETCs bring large accumulated rainfall totals and extensive flooding in GB [63, 66, 69]. Thus, our evidence of coincident *widespread* flood and wind on the same day in 5 out of 10 years and within 13 days in another 4 of those years contradicts a prevailing view that storms such as Desmond was exceptional in bringing both very severe wind and widespread flooding [3, 59]. These findings also highlight the importance of considering longer time-lags when assessing dependencies between weather-driven hazards where both may not occur in the same defined extreme episode. As far we are aware, this is the first statistical evidence of a time-lagged link between widespread flooding and severe wind for any nation. Our methodology also enables potential detection of such inter-dependencies elsewhere.

One implication of coincident floods and severe winds is that worst-case years are likely more severe than previously thought. With the association apparently strongest for the most extreme episodes, the effect of this co-occurrence likely increases combined flood-wind insurance losses for domestic UK properties in bad years [35]. Moreover, GB is located beneath the North Atlantic storm track and is, therefore, affected by the passage of ETCs [66] which bring extreme winds [68] that can subsequently affect central Europe [63, 70]. Since ETCs can continue to strengthen after landfall, this effect may extend to a much larger

physical and financial scale than the GB alone. Furthermore, there is a likely three-way association between widespread flooding, severe wind *and* storm surges that warrants investigation.

### 5.4. Operational implications

The Environment Agency is responsible for contingency planning, forecasting and managing the consequences of widespread flood episodes. Regional ‘footprints’ of past severe episodes (figure 2) reveal the extent to which authorities in neighbouring areas could be impacted simultaneously. This is relevant when coordinating and sharing equipment and personnel during such episodes. For instance, the Midlands region of the Environment Agency lies in a pivotal location since it may be called upon to provide resources to affected areas to the North and South. During the severe flooding in December 2015, personal and equipment were drawn from regions hundreds of kilometres away from the epicentre of Northwest England and Southern Scotland. This might not be feasible in the event of a MBF episode on the scale of January/February 1995 (figure 2(f)). However, knowledge of the likelihood and pattern of MBF provides a basis for role-play exercises as part of the contingency planning for such episodes.

Both the UK National Flood Resilience Review [71] and UK Climate Change Risk Assessment [2] recognise interdependencies between critical networks (e.g. electricity, water and transport) and the need to manage indirect flood impacts on the economy. However, their emphasis remains on integrated, yet single-basin solutions involving ‘natural’ flood management, improved property- and asset-level resilience, and planning controls. Widespread flooding in Australia in 2011, and multiple events in Central Europe since 2002, show the need for a higher-level strategy for managing extensive, transboundary flooding [72]. Moreover, the likelihood of MBF could increase with ETCs intensity and ARs frequency and magnitude expected to rise under anthropogenic climate change [49, 66, 70, 73–75].

### Acknowledgments

The authors thank the Scottish Environment Protection Agency for providing Scottish peak flow data, the Centre for Ecology and Hydrology for the SPI data, Swen Brands for providing the AR array along with detailed information, the RCUK (CENTA NERC) for the funding availability, the editor and two anonymous referees for their constructive comments. The authors declare no competing financial interests.

### ORCID iDS

Paolo De Luca  <https://orcid.org/0000-0002-0416-4622>

## Appendix

Table of Notation Acronyms used within the text and full definition.

Acronym	Definition	Unit
A	basin area	km <sup>2</sup>
AMAX	peak flow annual maximum	m <sup>3</sup> s <sup>-1</sup>
ARs	atmospheric rivers	kg m <sup>-1</sup> s <sup>-1</sup> (integrated horizontal water vapour transport, IVT)
d <sub>max</sub>	the last day of a multi-basin flooding episode, where the largest number of basins recorded their AMAX	day
ETCs	extra-tropical cyclones	–
FY	Flood Yield	m <sup>3</sup> s <sup>-1</sup> km <sup>-2</sup>
F-Index	Flood Index	–
GB	Great Britain	–
HAs	hydrometric areas	–
Jt	joining time	days
L	time window	days
LWTs	Lamb Weather Types	–
MBF	multi-basin flooding	–
mFY	multi-basin Flood Yield	m <sup>3</sup> s <sup>-1</sup> km <sup>-2</sup>
n <sub>g</sub>	metric with severity based on the number of basins concurrently reaching their AMAX within a given time window	–
SPI	Standardized Precipitation Index	units of standard deviation
T <sub>p</sub>	time to peak	hours
TDA	total drained area	km <sup>2</sup>
VSG	Very Severe Gales	G > 50 (G = gale index) [48]

## References

- [1] UNISDR (United Nations International Strategy for Disaster Reduction) 2015 *Sendai framework for disaster risk reduction 2015–2030*
- [2] ASC 2016 UK Climate Change Risk Assessment 2017 Synthesis Report: priorities for the next five years *Adaptation Sub-Committee of the Committee on Climate Change, London*
- [3] Barker L, Hannaford J, Muchan K, Turner S and Parry S 2016 The winter 2015/2016 floods in the UK: a hydrological appraisal *Weather* **71** 324–33
- [4] Muchan K, Lewis M, Hannaford J and Parry S 2015 The winter storms of 2013/2014 in the UK: hydrological responses and impacts *Weather* **70** 55–61
- [5] Parry S, Marsh T and Kendon M 2013 2012: From drought to floods in England and Wales *Weather* **68** 268–74
- [6] Marsh T 2008 A hydrological overview of the summer 2007 floods in England and Wales *Weather* **63** 274–9
- [7] Merz R and Blöschl G 2003 A process typology of regional floods *Water Resour. Res.* **39** 1–20
- [8] Nied M, Schröter K, Lüdtko S, Dung Nguyen V and Merz B 2016 What are the hydro-meteorological controls on flood characteristics? *J. Hydrol.* **545** 310–26
- [9] Gaail L, Szolgay J, Hlavčová K, Parajka J, Viglione A, Merz R and Blöschl G 2015 Dependence between flood peaks and volumes: a case study on climate and hydrological controls *Hydrol. Sci. J.* **60** 968–84
- [10] Viglione A, Chirico G B, Komma J, Woods R, Borga M and Blöschl G 2010 Quantifying space-time dynamics of flood event types *J. Hydrol.* **394** 213–29
- [11] Blöschl G *et al* 2015 Increasing river floods: fiction or reality? *Wiley Interdiscip. Rev. Water* **2** 329–44
- [12] Huntingford C *et al* 2014 Potential influences on the United Kingdom's floods of winter 2013/14 *Nat. Clim. Change* **4** 769–77
- [13] Schaller N *et al* 2016 Human influence on climate in the 2014 southern England winter floods and their impacts *Nat. Clim. Change* **6** 627–34
- [14] Mallakpour I and Villarini G 2015 The changing nature of flooding across the central United States *Nat. Clim. Change* **5** 250–4
- [15] Merz B *et al* 2014 Floods and climate: emerging perspectives for flood risk assessment and management *Nat. Hazards Earth Syst. Sci.* **14** 1921–42
- [16] Kjeldsen T R and Jones D A 2009 A formal statistical model for pooled analysis of extreme floods *Hydrol. Res.* **40** 465–80
- [17] Cunderlik J M and Burn D H 2003 Non-stationary pooled flood frequency analysis *J. Hydrol.* **276** 210–23
- [18] Heffernan J E and Tawn J A 2004 A conditional approach for multivariate extreme values *J. R. Stat. Soc. Ser. B Stat. Methodol.* **66** 497–530
- [19] Keef C, Svensson C and Tawn J A 2009 Spatial dependence in extreme river flows and precipitation for Great Britain *J. Hydrol.* **378** 240–52
- [20] Keef C, Tawn J A and Lamb R 2013 Estimating the probability of widespread flood events *Environmetrics* **24** 13–21
- [21] De Waal D J, Van Gelder P H A J M and Nel A 2007 Estimating joint tail probabilities of river discharges through the logistic copula *Environmetrics* **18** 621–31
- [22] Chen L, Singh V P, Shenglian G, Hao Z and Li T 2012 Flood coincidence risk analysis using multivariate copula functions *J. Hydrol. Eng.* **17** 742–55
- [23] Wyncoll D and Gouldby B 2013 Integrating a multivariate extreme value method within a system flood risk analysis model *J. Flood Risk Manage.* **8** 145–60
- [24] Qu Y, Dodov B, Jain V and Hautaniemi T 2010 An inland flood loss estimation model for Great Britain *British Hydrological Society 3rd International Symposium, Managing Consequences of a Changing Global Environment*, 19–23 July
- [25] Sampson C C, Fewtrell T J, O'Loughlin F, Pappenberger F, Bates P B, Freer J E and Cloke H L 2014 The impact of uncertain precipitation data on insurance loss estimates using a flood catastrophe model *Hydrol. Earth Syst. Sci.* **18** 2305–24
- [26] Ghizzoni T, Roth G and Rudari R 2012 Multisite flooding hazard assessment in the upper Mississippi river *J. Hydrol.* **412–413** 101–13
- [27] Ghizzoni T, Roth G and Rudari R 2010 Multivariate skew-t approach to the design of accumulation risk scenarios for the flooding hazard *Adv. Water Resour.* **33** 1243–55
- [28] Cameron D S, Beven K J, Tawn J, Blazkova S and Naden P 1999 Flood frequency estimation by continuous simulation for a gauged upland catchment (with uncertainty) *J. Hydrol.* **219** 169–87
- [29] Lamb R 2006 Rainfall-runoff modelling for flood frequency estimation *Encycl. Hydrolog. Sci.* **11** 125
- [30] Lamb R, Keef C, Tawn J, Laeger S, Meadowcroft I, Surendran S, Dunning P and Bastone C 2010 A new method to assess the risk of local and widespread flooding on rivers and coasts *J. Flood Risk Manage.* **3** 323–36

- [31] Uhlemann S, Thielen A H and Merz B 2010 A consistent set of trans-basin floods in Germany between 1952–2002 *Hydrol. Earth Syst. Sci.* **14** 1277–95
- [32] Uhlemann S, Thielen A H and Merz B 2014 A quality assessment framework for natural hazard event documentation: application to trans-basin flood reports in Germany *Nat. Hazards Earth Syst. Sci.* **14** 189–208
- [33] Jongman B, Hochrainer-Stigler S, Feyen L, Aerts J C J H, Mechler R, Botzen W J W, Bouwer L M, Pflug G, Rojas R and Ward P J 2014 Increasing stress on disaster-risk finance due to large floods *Nat. Clim. Change* **4** 264–8
- [34] Lavers D A, Allan R P, Wood E F, Villarini G, Brayshaw D J and Wade A J 2011 Winter floods in Britain are connected to atmospheric rivers *Geophys. Res. Lett.* **38** 1–8
- [35] Hillier J K, Macdonald N, Leckebusch G C and Stavriniades A 2015 Interactions between apparently ‘primary’ weather-driven hazards and their cost *Environ. Res. Lett.* **10** 104003
- [36] Perry A H 1980 A note on the south Wales floods of late December 1979 *Weather* **35** 106–9
- [37] Kelman I 2001 The autumn 2000 floods in England and flood management *Weather* **56** 346–60
- [38] Marsh T J and Dale M 2002 The UK floods of 2000–2001: a hydrometeorological appraisal *Water Environ. J.* **16** 180–8
- [39] Environment Agency 2003 New Year Floods *FloodLink*
- [40] Meteorological Office 1992 *Monthly Weather Report* **109**
- [41] Hulme M 1997 The climate in the UK from November 1994 to October 1995 *Weather* **52** 242–57
- [42] Watkins S and Whyte I 2008 Extreme flood events in upland catchments in Cumbria since 1600: the evidence of historical records *North West Geogr.* **8** 1
- [43] Wilby R L and Quinn N W 2013 Reconstructing multi-decadal variations in fluvial flood risk using atmospheric circulation patterns *J. Hydrol.* **487** 109–21
- [44] Kendon M and McCarthy M 2015 The UK’s wet and stormy winter of 2013/2014 *Weather* **70** 40–7
- [45] Wallingford Hydrosolutions 2016 *The Revitalised Flood Hydrograph Model ReFH 2.2: Technical Guidance* (Wallingford: Wallingford Hydrosolutions and the Centre for Ecology & Hydrology)
- [46] Wallingford: Centre for Ecology & Hydrology 2009 FEH CD-ROM 3
- [47] Lamb H H 1972 British Isles weather types and a register of the daily sequence of circulation patterns *Geophysical Memoirs* vol 116 (London: HMSO)
- [48] Jones P D, Harpham C and Briffa K R 2013 Lamb weather types derived from reanalysis products *Int. J. Climatol.* **33** 1129–39
- [49] Lavers D A, Allan R P, Villarini G, Lloyd-Hughes B, Brayshaw D J and Wade A J 2013 Future changes in atmospheric rivers and their implications for winter flooding in Britain *Environ. Res. Lett.* **8** 034010
- [50] Brands S, Gutiérrez J M and San-Martín D 2017 Twentieth-century atmospheric river activity along the west coasts of Europe and North America: algorithm formulation, reanalysis uncertainty and links to atmospheric circulation patterns *Clim. Dyn.* **48** 2771–95
- [51] Dee D P *et al* 2011 The ERA-Interim reanalysis: configuration and performance of the data assimilation system *Q. J. R. Meteorol. Soc.* **137** 553–97
- [52] Berghuijs W R, Woods R A, Hutton C J and Sivapalan M 2016 Dominant flood generating mechanisms across the United States *Geophys. Res. Lett.* **43** 4382–90
- [53] McKee T B, Doesken N J and Kleist J 1993 The relationship of drought frequency and duration to time scales *8th AMS Conference on Applied on Climatology*, 17–22 January
- [54] McKee T B, Doesken N J and Kleist J 1995 Drought monitoring with multiple time scales *9th AMS Conference on Applied Climatology*, 15–20 January
- [55] Seiler R A, Hayes M and Bressan L 2002 Using the standardized precipitation index for flood risk monitoring *Int. J. Climatol.* **22** 1365–76
- [56] Du J, Fang J, Xu W and Shi P 2013 Analysis of dry/wet conditions using the standardized precipitation index and its potential usefulness for drought/flood monitoring in Human Province, China *Stoch. Environ. Res. Risk Assess.* **27** 377–87
- [57] Wang Y, Chen X, Chen Y, Liu M and Gao L 2015 Flood/drought event identification using an effective indicator based on the correlations between multiple time scales of the Standardized Precipitation Index and river discharge *Theor. Appl. Climatol.* **128** 159–68
- [58] Tanguy M, Kral F, Fry M, Svensson C and Hannaford J 2015 Standardised Precipitation Index time series for Integrated Hydrological Units Hydrometric Areas 1961–2012 *NERC Environmental Information Data Centre*
- [59] McCarthy M, Spillane S, Walsh S and Kendon M 2016 The meteorology of the exceptional winter of 2015/2016 across the UK and Ireland *Weather* **71** 305–13
- [60] Befort D J, Wild S, Kruschke T, Ulbrich U and Leckebusch G C 2016 Different long-term trends of extra-tropical cyclones and windstorms in ERA-20C and NOAA-20CR reanalyses *Atmos. Sci. Lett.* **17** 586–95
- [61] Wild S, Befort D J and Leckebusch G C 2015 Was the extreme storm season in winter 2013/14 over the North Atlantic and the United Kingdom triggered by changes in the West Pacific warm pool? *Bull. Am. Meteorol. Soc.* **96** 29–34
- [62] Matthews T, Murphy C, Wilby R L and Harrigan S 2014 Stormiest winter on record for Ireland and UK *Nat. Clim. Change* **4** 738–40
- [63] Priestley M D K, Pinto J G, Dacre H F and Shaffrey L C 2017 The role of cyclone clustering during the stormy winter of 2013/2014 *Weather* **72** 187–92
- [64] Pattison I and Lane S N 2012 The relationship between Lamb weather types and long-term changes in flood frequency, River Eden, UK *Int. J. Climatol.* **32** 1971–89
- [65] Hannaford J and Marsh T J 2008 High-flow and flood trends in a network of undisturbed catchments in the UK *Int. J. Climatol.* **28** 1325–38
- [66] Matthews T, Murphy C, Wilby R L and Harrigan S 2016 A cyclone climatology of the British-Irish Isles 1871–2012 *Int. J. Climatol.* **36** 1299–312
- [67] Grimaldi S, Petroselli A, Tauro F and Porfiri M 2012 Time of concentration: a paradox in modern hydrology *Hydrol. Sci. J.* **2** 217–28
- [68] Pinto J G, Zacharias S, Fink A H, Leckebusch G C and Ulbrich U 2009 Factors contributing to the development of extreme North Atlantic cyclones and their relationship with the NAO *Clim. Dyn.* **32** 711–37
- [69] Burt T P, Jones P D and Howden N J K 2015 An analysis of rainfall across the British Isles in the 1870s *Int. J. Climatol.* **35** 2934–47
- [70] Donat M G, Leckebusch G C, Pinto J G and Ulbrich U 2010 Examination of wind storms over Central Europe with respect to circulation weather types and NAO phases *Int. J. Climatol.* **30** 1289–300
- [71] HM Government 2016 National Flood Resilience Review 145pp
- [72] Wilby R L and Keenan R 2012 Adapting to flood risk under climate change *Prog. Phys. Geogr.* **36** 348–78
- [73] Ulbrich U, Leckebusch G C and Pinto J G 2009 Extra-tropical cyclones in the present and future climate: a review *Theor. Appl. Climatol.* **96** 117–31
- [74] Zappa G, Shaffrey L C, Hodges K I, Sanson P G and Stephenson D B 2013 A multimodel assessment of future projections of north atlantic and european extratropical cyclones in the CMIP5 climate models *J. Clim.* **26** 5846–62
- [75] Donat M G, Leckebusch G C, Pinto J G and Ulbrich U 2010 European storminess and associated circulation weather types: future changes deduced from a multi-model ensemble of GCM simulations *Clim. Res.* **42** 27–43